Simultaneous Biplane First-Pass Radionuclide Angiocardiography Using a Scintillation Camera with Two Perpendicular Detectors

E. Gordon DePuey, Helen Salensky, Steven Melancon and Kenneth J. Nichols

Department of Radiology, Division of Nuclear Medicine, and Department of Internal Medicine, Division of Cardiology, St. Luke's-Roosevelt Hospital Center and Columbia University College of Physicians and Surgeons, New York, New York

Generally performed in a single anterior or right anterior oblique (RAO) view, first-pass radionuclide angiocardiography (RNA) is limited due to its inability to evaluate septal and posterior wall motion. **Methods:** Thirty-five patients undergoing stress/rest sestamibi SPECT (22 mCi/22 mCi 2-day protocol) underwent biplane RNA at the time of resting injection. The stress SPECT images (acquired with the patient at rest) were ECG-gated to evaluate resting regional myocardial wall thickening. By this means wall motion assessed by RNA was compared to the presence of a resting SPECT perfusion defect accompanied by a localized decrease in wall thickening. **Results:** In 16 patients in whom both resting perfusion and wall thickening were normal, one demonstrated apical hypokinesis by RNA in the RAO view. In the other 29 patients, a total of 58 resting segmental perfusion defects with abnormal wall thickening were present (12 anterior, 13 inferior, 14 apical, 11 septal and 8 posterolateral). Wall motion abnormalities were detected in all these patients and in 57/58 segments (98%) by biplane RNA. Septal and posterolateral wall motion abnormalities were detected in only the LAO RNA study. In three patients, wall motion abnormalities were detected by LAO imaging only. Of the remaining 87 normally perfused segments in these 29 patients, RNA wall motion was normal in 85. Two posterolateral segments demonstrated apparent hypokinesis, probably due to left atrial overlap in the LAO projection. **Conclusion:** Simultaneous biplane RNA accurately detects wall motion abnormalities frequently missed by single-plane RAO imaging.

Key Words: first-pass radionuclide angiocardiography; ventricular function; technetium-99m-sestamibi; scintillation camera

J Nucl Med 1994; 35:1593–1601

First-pass radionuclide angiocardiography (RNA) is performed in a single planar projection, usually the anterior or right anterior oblique (RAO) view. The accuracy of RNA to determine left ventricular ejection fraction (LVEF) and evaluate regional wall motion has been well documented for both multicrystal (*1*) and single-crystal (*2*) scintillation detector systems. However, evaluation of regional wall motion is limited using single-plane first-pass RNA. In the anterior or RAO projection it is not possible to adequately evaluate the septum and posterior wall. To assess septal and posterior wall motion, repeat imaging in the left anterior oblique (LAO) view is necessary, following a second injection of radiotracer. Recently, several single-crystal scintillation cameras have become commercially available potentially enabling simultaneous biplane first-pass RNA.

The purpose of the present study was to determine the feasibility of performing simultaneous biplane first-pass RNA on a two-headed detector system. Regional wall motion of all ventricular segments was evaluated subjectively by visual analysis, and regional ejection fraction was determined by a standard quantitative count rate-based method. It has been previously established that fixed myocardial perfusion defects are nearly always accompanied by regional wall motion abnormalities (*3,4*). In this study of 35 patients, regional dysfunction present on biplane first-pass RNA was correlated with the presence of myocardial perfusion defects accompanied by decreased wall thickening as determined by ^{99m}Tc-sestamibi gated SPECT.

MATERIALS AND METHODS

Patient Population

Thirty-five adult patients (21 males, 14 females, mean age ± 1 s.d.; 59 ± 13 yr) were studied. Eighteen patients had sustained prior myocardial infarction, documented historically and/or electrocardiographically, and were referred to the Nuclear Medicine Laboratory for stress myocardial perfusion imaging to evaluate the possibility of myocardial ischemia. The remaining 17 patients were referred for stress perfusion imaging because of a moderate

Received Nov. 22, 1993; revision accepted May 5, 1994.

For correspondence and reprints contact: E. Gordon DePuey, MD, St. Luke's-Roosevelt Hospital Center, Amsterdam Avenue at 114th St., New York, NY 10025.

to high (≥ 50%) likelihood of coronary disease based upon risk factors. All patients were clinically stable, and none had sustained a cardiac event within the past 6 wk.

Scintillation Camera with Two Perpendicular Detectors

The dual-scintillation detector system used for this study is commercially available (Optima, General Electric Medical Systems, Milwaukee, WI) and consists of two perpendicular rectangular single-crystal sodium iodide detectors, each measuring 350 × 190 mm (useful field of view). The detectors are joined along the shorter dimension at a 90° angle in a fixed geometry.

The functional parameters of similar electronics and ultrahigh sensitivity collimators for a 400-mm diameter single-detector camera have been reported previously as applied to first-pass RNA (*5*). Compared to conventional single-crystal detectors, the improved electronics are capable of increasing sensitivity by a factor of 2.6 (*6*), and the ultrahigh sensitivity collimator is 4.7 times more sensitive than a similar general purpose collimator. For ^{99m}Tc in a 20% symmetric window, the rectangular detector exhibited a 20% count rate loss at 195 kcps, and the absolute maximum received count rate was observed to be 275 kcps, beyond which the detector can be completely paralyzed. As a point of reference, the maximum count rate capability of the first generation multicrystal cameras was 250 kcps, and that of the newest generation multicrystal cameras is approximately 1,000 kcps.

Myocardial Perfusion Imaging

Rest/stress myocardial perfusion imaging was performed in all patients using ^{99m}Tc-sestamibi. A separate-day imaging protocol was used. Each patient was intravenously administered 22 mCi ^{99m}Tc-sestamibi at rest, and nongated SPECT was performed 90 min later. On a second day, in almost all cases the next working day, a second 22-mCi dose was administered during peak exercise (19 patients) or pharmacologic stress (dipyridamole 0.52 μgm/kg given over 4 min in 16 patients). Stress gated SPECT images were acquired with the patient at rest beginning 20–30 min following radiopharmaceutical injection in conjunction with treadmill exercise or at 60–90 min in conjunction with dipyridamole stress.

The stress ^{99m}Tc-sestamibi SPECT images, acquired with the patient at rest, were ECG-gated in order to evaluate stress myocardial perfusion distribution and resting left ventricular function simultaneously. Eight frames per cardiac cycle were acquired. The resting ^{99m}Tc-sestamibi SPECT images were not gated. One-pixel (approximately 6.4 mm) thick myocardial slices were reconstructed in the short-axis, vertical long-axis and horizontal long-axis planes. Polar map reconstruction and comparison to gender-matched normal limits were performed using a commercially available software program (CEqual, General Electric Medical Systems, Milwaukee, WI).

All reconstructed tomographic images were viewed in both black and white and color at the computer console. A myocardial perfusion defect was judged to be present if a localized decrease in count density was observed in all three orthogonal tomographic planes as well as the polar coordinate map and was identified as abnormal (blackened) by quantitative analysis. Both the stress and rest SPECT images were evaluated in this fashion. Defects were judged to be reversible, partially reversible or fixed. However, for the purposes of the present study in which first-pass RNA resting wall motion was evaluated, the presence of a resting perfusion defect was of paramount importance.

Regional wall thickening was evaluated from the stress gated ^{99m}Tc-sestamibi SPECT images, viewed in endless-loop cinematic format in both black and white and color at the computer console. Wall thickening, assessed by the increase in regional image intensity during ventricular systole (*7*), was arbitrarily judged to be normal in the myocardial region with the greatest count density at end systole. The increase in count density was subjectively assessed by the increase in image intensity on the computer color monitor. Regions with less than 50% of normal systolic thickening were judged to be abnormal.

For the localization of perfusion defects and the assessment of wall thickening, the left ventricle was divided into five regions—the anterior wall, apex, inferior wall, septum and posterolateral wall. Although tomography allowed more precise localization of abnormalities, since comparison was made to planar RNA, only these five relatively large regions were evaluated.

First-Pass Radionuclide Angiocardiography

At the time of the resting injection of 22 mCi of ^{99m}Tc-sestamibi injection, biplane first-pass RNA was performed. Patients were positioned supine on the SPECT imaging palette. Scintillation Detector 2 was placed over the precordium in the 30° RAO position so that the left ventricle was estimated to be centered within the field of view. By virtue of the perpendicular orientation of the two detectors, Detector 1 was by definition in the 60° LAO position. The dual-detector camera was initially positioned so that Detector 2 was against the chest wall in the RAO projection. The detectors were then raised as a unit so that the heart was approximately in the center of the long axis of both detectors. Positioning of the heart within the center of the fields of view was confirmed using a ^{57}Co sheet source transmission image. Camera positioning by this means was easily accomplished with adequate visualization of the left and right ventricles in both the RAO and LAO views following subsequent tracer injection, even in patients with cardiomegaly.

The ^{99m}Tc-sestamibi dose was loaded into a segment of intravenous extension tubing and subsequently injected as a compact bolus (< 0.5 cc) into the patient's right antecubital vein as rapidly as possible via an 18-gauge indwelling intravenous catheter, followed by a 20-cc saline flush. To help assure a compact bolus and to avoid performing a Valsalva maneuver, patients were instructed to breathe normally.

For data acquisition, a 30% energy window (± 15%) was centered on the 140-keV ^{99m}Tc photopeak. Ultrahigh-sensitivity collimators were used for each detector. First-pass data were acquired in 64 × 64 matrices for 1200 frames over 30 sec. By means of ECG gating, R-wave trigger information was acquired simultaneously with the images.

Data processing for this high sensitivity camera/collimator system has been described previously (*5*). In summary, images were first reframed at 0.1 sec. Bolus integrity was evaluated from a time-activity curve from the superior vena cava. In all patients included in this study, bolus transit time was < 1.5 sec and was thereby judged to be adequate. From reframed images, an initial left ventricular time-activity curve was generated with R-wave trigger marks superimposed. From this time-activity curve, arrhythmic R-R intervals falling ± 10% outside of the average R-R interval were excluded and cardiac cycles from the left ventricular phase of the time-activity curve were selected automatically with subsequent operator confirmation. From the complete 1200-frame dataset, a filtered representative 12 frame per cardiac cycle image was generated corresponding to the accepted representative heartbeats within the left ventricular phase of the time-activity curve. A "lung method" of background subtraction was used whereby counts were subtracted in varying degrees throughout

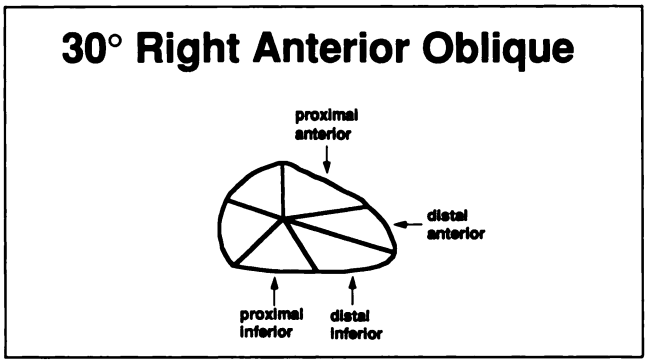

FIGURE 1. Segments used for analysis of RAO first-pass RNA regional ejection fraction.

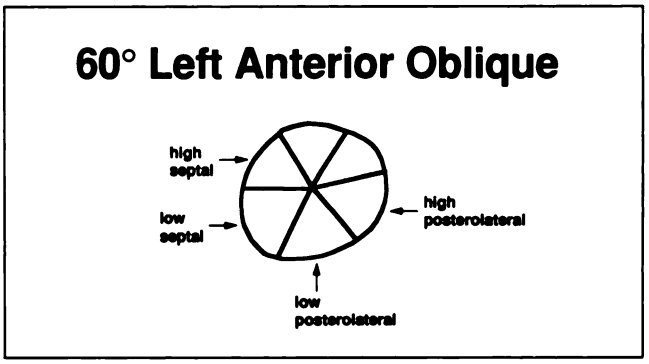

FIGURE 2. Segments used for analysis of LAO first-pass RNA regional ejection fraction.

the left ventricular phase based on the presence of lung counts before and during the left ventricular phase. By this means RAO and LAO first-pass RNA images were obtained and displayed in endless loop cinematic format in both color and black and white on the computer monitors.

Guided by end-diastolic, end-systolic, phase and amplitude images, an observer then manually refined the end-diastolic and end-systolic left ventricular regions of interest (ROIs) (if necessary) using the RAO and LAO representative cycle images. Cine RAO and LAO images were displayed with and without the user-defined, end-diastolic reference outlines. From the redefined regions, left ventricular ejection fraction was calculated from the RAO view using a standard background-subtracted count rate-based method. Color-coded regional RAO and LAO ejection fraction functional images were displayed.

By subjective visual analysis, a first-pass RNA wall motion abnormality was judged to be present if regional wall excursion was unequivocally reduced and if an abnormality was defined on the regional ejection fraction image. Wall motion of the anterior wall, apex and inferior walls was assessed from the RAO image. Posterolateral and septal wall motion was evaluated from the LAO image.

Regional ejection fractions were also calculated from four segments in the RAO view (proximal anterior, distal anterior, proximal inferior and distal inferior) (Fig. 1) and from four segments in the LAO view (high septal, low septal, high posterolateral and low posterolateral) (Fig. 2).

Comparison of SPECT Perfusion and First-Pass RNA Data

Apparent perfusion defects may result from localized soft tissue attenuation, particularly due to the left breast and left hemidiaphragm. Moreover, small transmural infarcts and subendocardial scarring may create perfusion defects but may not necessarily result in regional wall motion abnormalities. Therefore, since the purpose of the present study was to document wall motion abnormalities assessed by first-pass RNA and compare them to definite SPECT perfusion scan findings, we required that a perfusion defect be accompanied by a significant decrease in myocardial wall thickening to be used as a comparator. Thus, the sensitivity and specificity of simultaneous biplane first-pass RNA in detecting regional dysfunction were determined by comparison to the presence of a resting SPECT perfusion defect accompanied by a decrease in regional myocardial wall thickening. Such analysis was performed to evaluate the technique in individual patients and also individual myocardial segments. First-pass RNA and gated perfusion SPECT were interpreted independently on separate days. To determine the diagnostic performance characteristics of a more objective RNA assessment of regional function, namely regional ejection fraction, this parameter was also evaluated. However, since the apex of the left ventricle is not exclusively encompassed in any computer-defined region from which we calculated regional ejection fraction, such analysis could not be performed for the apex.

All values quoted are the mean ± 1 standard deviation. The Student's t-test for unpaired data was used to compare regional ejection fraction results among patients.

RESULTS

Sequential reframed, 1 sec per frame RAO and LAO first-pass images from a representative normal study are shown in Figure 3. The corresponding time-activity curves from ROIs over the left ventricular cavity (1200 frames in 30 sec) are shown in Figure 4.

Resting ^{99m}Tc-sestamibi SPECT was normal in 16 of the 35 patients. In five other patients, mild to moderate fixed defects were present in the apex (1 male), anterior wall (2 females) and inferior wall (1 male). However, gated SPECT demonstrated entirely normal wall thickening in the distribution of these fixed defects, and the patients had no historical or electrocardiographic evidence of prior infarction. The fixed defects in these five patients were therefore judged to be due to physiologic apical "thinning," breast attenuation and diaphragmatic attenuation respec-

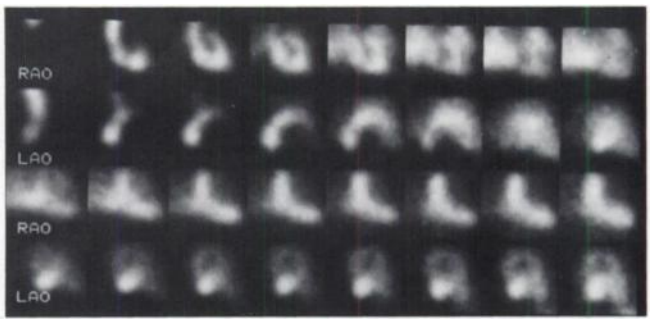

FIGURE 3. Reframed, one frame per second, first-pass RNA images in the RAO and LAO views from a representative normal study.

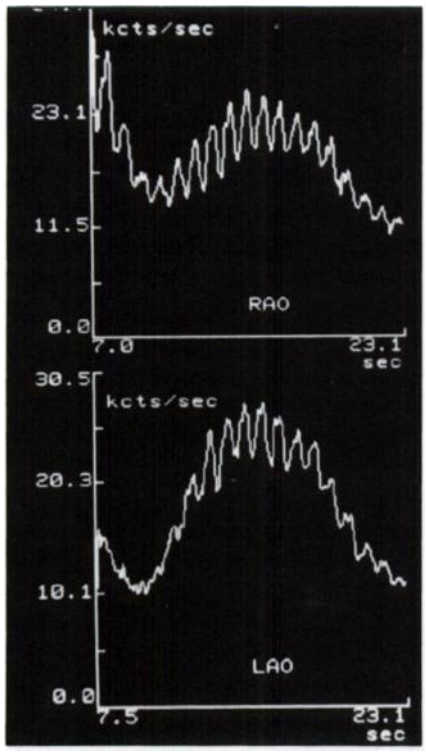

FIGURE 4. Time-activity curves from ROIs placed over the entire left ventricular cavity in the RAO and LAO projections.

tively. In these 16 patients judged to have normal ^{99m}Tc-sestamibi SPECT, first-pass RNA demonstrated mild to moderate apical hypokinesis in the RAO view in one patient. Otherwise regional wall motion was normal (94% patient specificity).

Resting perfusion defects associated with decreased wall thickening were present in one or more myocardial segments in the other 19 patients. One or more regional wall motion abnormalities were present on first-pass RNA in each of these 16 patients (100% patient sensitivity). A total of 58 resting segmental perfusion defects were present (Table 1). Perfusion defects were fixed in 41 segments and partially reversible in 17 segments. Visual assessment of first-pass RAO RNA demonstrated abnormal wall motion in 12 of 12 anterior perfusion defects, 14 of 14 apical defects, and 12 of 13 inferior defects. The single resting inferior perfusion defect with decreased wall thickening which failed to demonstrate regional asynergy by RNA was fixed, of moderate severity and involved the mid and distal inferior wall.

Septal or posterior abnormalities were frequent, occurring in 17 of 19 patients (89%) with abnormal ^{99m}Tc-sestamibi SPECT. Associated wall motion abnormalities were detected by first-pass RNA in only the LAO projection. Visual assessment of first-pass RNA in the LAO projection demonstrated wall motion abnormalities associated with septal perfusion defects with abnormal wall thickening in 11 of 11 segments. In all such cases septal asynergy was associated with additional anterior and/or apical abnormalities and occurred in patients with prior anterio/anteroseptal myocardial infarction.

Posterolateral wall motion abnormalities were observed in 8 of 8 patients with resting posterolateral perfusion defects and decreased wall thickening. In 5 patients these were accompanied by inferior abnormalities in patients with inferior/inferolateral infarction, although in two of these patients the posterior wall motion abnormalities were much more marked than the inferior abnormalities. However, in the other 3 patients the posterolateral abnormalities were isolated (normal RAO wall motion) and associated with posterior or lateral wall infarction, most likely due to left circumflex coronary artery disease. Posterolateral wall motion abnormalities were also present in two patients who had perfusion defects in other segments but in whom both posterolateral perfusion and wall thickening were normal. Retrospectively, in one patient the false-positive RNA finding was most likely due to overlap of the left atrium and the posterior wall of the left ventricle, giving the appearance of marked posterior hypokinesis as the left atrium filled during ventricular systole. No explanation could be found for the other false-positive posterolateral RNA finding. In these 19 patients myocardial perfusion, wall thickening and wall motion were normal in the remaining 94 segments. In all 35 patients, there was concordance between first-pass RNA wall motion and SPECT perfusion and wall thickening in 57 of 58 segments with perfusion defects (98% segmental sensitivity) and 219 of 222 segments with normal perfusion (99% segmental specificity).

A resting perfusion defect was strongly correlated with a decrease in regional ejection fraction. Anterior perfusion defects were associated with a percent regional ejection fraction of 41 ± 19 in the proximal anterior wall and 24 ± 15 in the distal anterior wall. These values were significantly lower than regional ejection fractions of normally perfused anterior segments (73 ± 20, $p = 0.00009$; and 73 ± 20, $p < 10^{-6}$ respectively) (Fig. 5). In patients with inferior perfusion defects, proximal and distal inferior regional ejection fractions were significantly lower than those of normally perfused inferior segments (43 ± 19 vs. 64 ± 21,

TABLE 1
Comparison of First-Pass RNA Segmental Wall Motion with ^{99m}Tc-Sestamibi SPECT Resting Perfusion Defects

	Resting SPECT Perfusion Defects				
	Anterior (n = 12)	Apical (n = 14)	Inferior (n = 13)	Septal (n = 11)	Postlateral (n = 8)
RAO FP abnormal	12	14	12	—	—
LAO FP abnormal	—	—	—	11	10

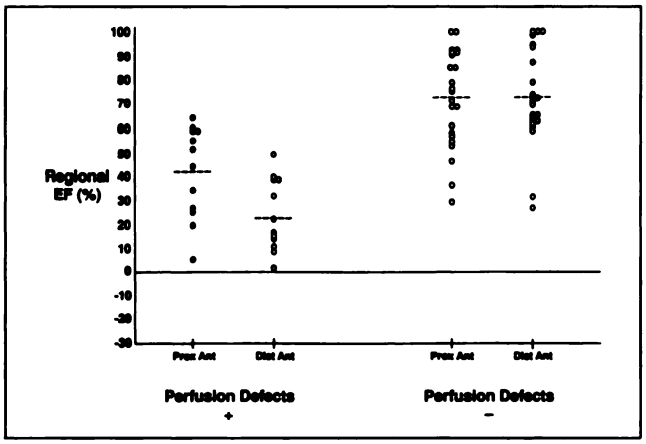

FIGURE 5. Anterior regional ejection fractions in myocardial segments with (+) and without (−) resting SPECT perfusion defects. Ant = anterior, Prox = proximal and Dist = distal.

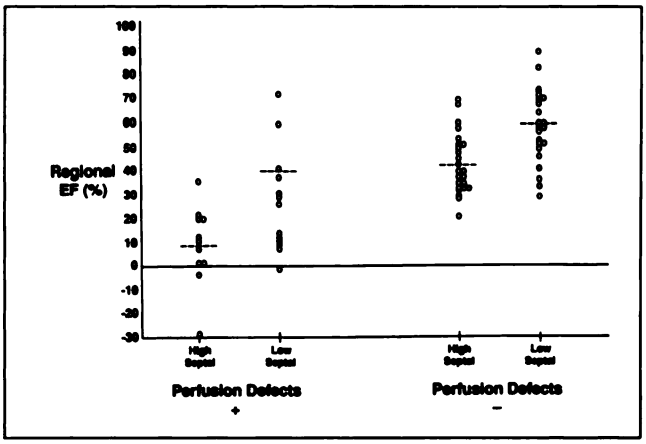

FIGURE 7. Septal regional ejection fractions in myocardial segments with (+) and without (−) resting SPECT perfusion defects.

p = 0.005; and 36 ± 24 vs. 73 ± 20, p = 0.00002) (Fig. 6). High septal and low septal regional ejection fractions were significantly lower in LAO first-pass RNA in abnormally perfused septal segments as compared to normal segments (8 ± 16 vs. 42 ± 12, $p < 10^{-6}$; and 19 ± 13 vs. 58 ± 15, $p < 10^{-6}$, respectively) (Fig. 7).

The most marked regional wall motion abnormalities and the lowest regional ejection fractions occurred in the septum. In three patients septal dyskinesis and a negative ejection fraction were observed. Regional ejection fraction differentiated normally versus abnormally perfused segments least well in the posterolateral wall. High posterolateral wall regional ejection fraction was 35 ± 14 in posterolateral segments with perfusion defects versus 46 ± 20 in posterolateral segments with normal perfusion (p = ns). Low posterolateral wall regional ejection fraction was 38 ± 20 and 46 ± 21 in abnormally versus normally perfused posterior segments, respectively (p = ns) (Fig. 8). Poor diagnostic performance of posterior regional ejection fraction was most likely due to the contribution of left atrial counts to the left ventricular posterior ROIs during ventricular systole in the 60° LAO view.

Examples

Patient 1: Normal. Left ventricular perfusion during exercise and at rest are normal (Fig. 9A), and wall motion and thickening are normal (Fig. 9B). In both the RAO (Fig. 9C) and LAO (Fig. 9D) projections, first-pass RNA reveals normal wall motion. The regional ejection fraction images in both projections are likewise normal. Global left ventricular ejection fraction calculated from the RAO study is 76%.

Patient 2: Anteroseptal Myocardial Infarction. In this 62-yr-old male, exercise and resting ^{99m}Tc-sestamibi SPECT demonstrated moderately severe fixed contiguous anterior, apical, inferoapical and septal perfusion defects (Fig. 10A). Wall thickening is moderately to markedly reduced in these regions (Fig. 10B). In the RAO view (Fig. 10C) anterior and apical wall motion abnormalities are present with an associated decrease in regional ejection fraction (19% proximal anterior, 10% distal anterior and

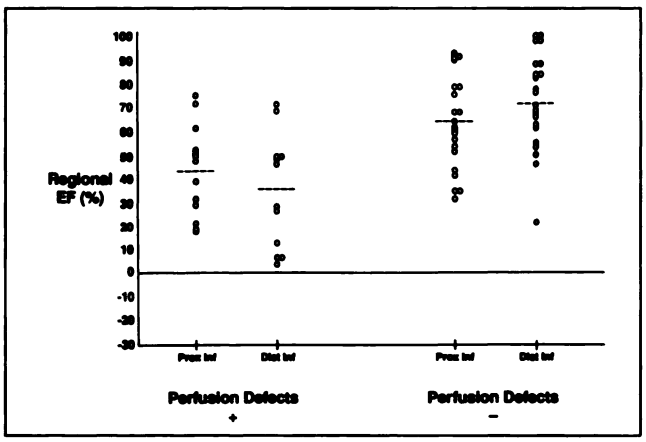

FIGURE 6. Inferior regional ejection fractions in myocardial segments with (+) and without (−) resting SPECT perfusion defects. Inf = inferior, prox = proximal, and dist = distal.

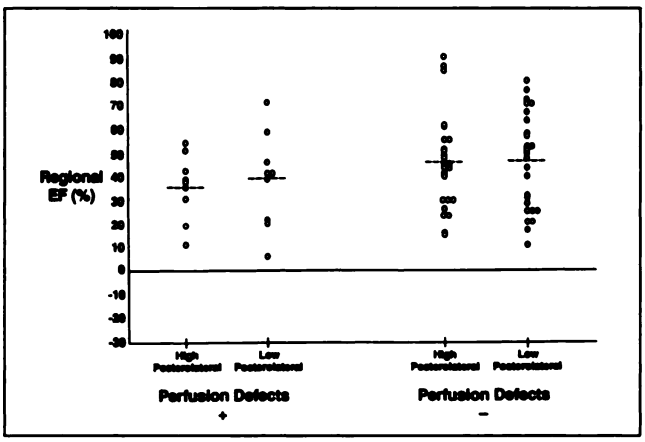

FIGURE 8. Posterolateral regional ejection fractions in myocardial segments with (+) and without (−) resting SPECT perfusion defects.

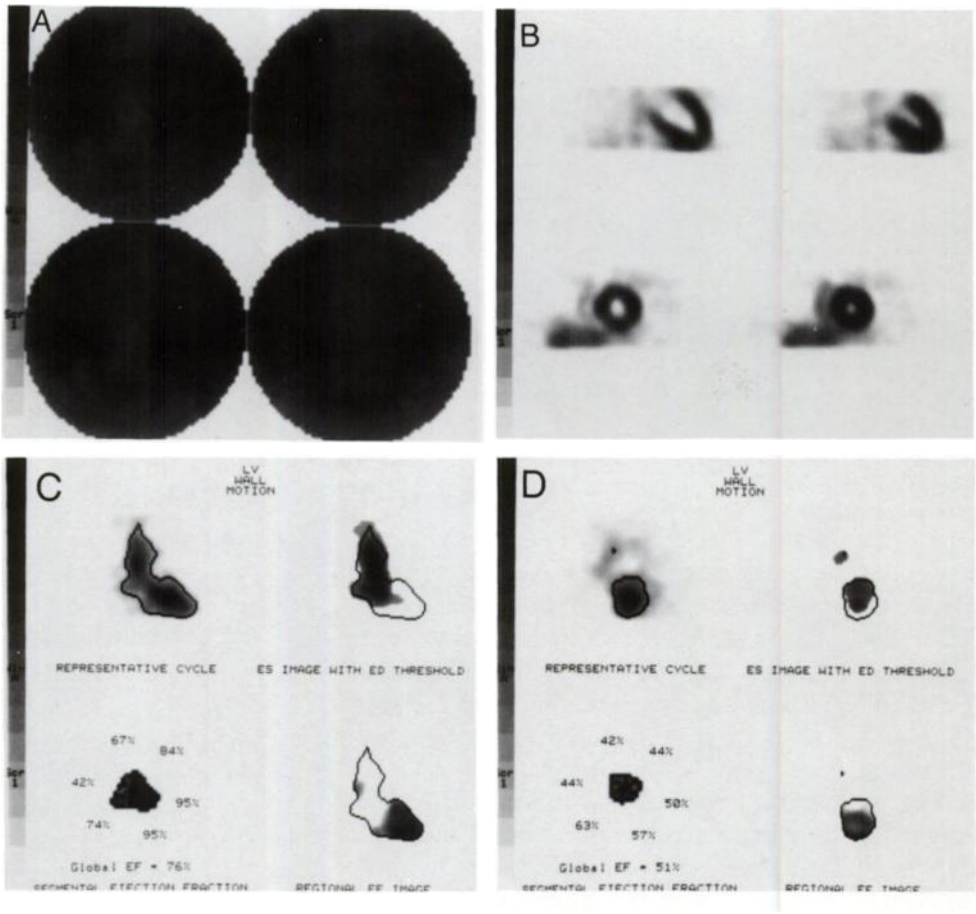

FIGURE 9. Normal ^{99m}Tc-sestamibi SPECT and biplane first-pass RNA. (A) Stress (left) and rest (right) raw polar plots (top row) demonstrate normal left ventricular perfusion. By quantitative analysis (below) no pixels are identified as abnormal. (B) End-diastolic (left) and end-systolic (right) tomographic slices in the vertical long-axis (top) and short-axis (bottom) projections demonstrated normal wall motion and wall thickening. (C) End-diastolic/end-systolic first-pass RNA RAO contours (top right) demonstrate normal wall motion. Regional ejection fractions (bottom left) are normal. The regional ejection fraction image (bottom right) also demonstrates normal, uniform function. (D) Analysis of LAO RNA data also demonstrates normal regional function.

27% distal inferior). In addition, the LAO first-pass RNA study (Fig. 10D) demonstrates septal asynergy and a marked decrease in regional ejection fraction (−31% high septum, 9% low septum). Global ejection fraction calculated from the RAO view is 28%. Thus, in this example the extent of regional asynergy would have been substantially underestimated without the simultaneous LAO first-pass RNA study.

Patient 3: Posterolateral Myocardial Infarction. This 50-yr-old male had no prior history of myocardial infarction, and his resting electrocardiogram was normal. He underwent dipyridamole stress and resting ^{99m}Tc-sestamibi SPECT to evaluate intermittent atypical chest pain. SPECT imaging demonstrated a partially reversible posterolateral perfusion defect, consistent with scar and superimposed ischemia in the left circumflex territory (Fig. 11A). Posterolateral wall thickening is moderately to markedly decreased (Fig. 11B). Wall motion as evaluated by first-pass RNA in the RAO view is normal (Fig. 11C). Global ejection fraction calculated from the RAO view is 57%. However, in the LAO view moderate to marked posterolateral hypokinesis is present as noted in the end-diastolic/end-systolic and regional ejection fraction images (Fig. 11D). High posterolateral ejection fraction is 18%. Thus, in this example the posterolateral infarct-related asynergy was demonstrable in only the LAO first-pass RNA study.

DISCUSSION

First-pass RNA is well established as a diagnostic test to measure left ventricular ejection fraction and evaluate regional wall motion. Resting and exercise function as evaluated by first-pass RNA provides important diagnostic and prognostic information useful in clinical decision making in patients with known or suspected coronary artery disease. Likewise, sequential studies have been valuable in assessing drug effects and medical and surgical interventions. However, since the technique is almost always performed in the anterior or RAO projection, its sensitivity in detecting septal and posterolateral asynergy is seldom reported. Bodenheimer et al. reported a decrease in sensitivity of first-pass RAO RNA in detecting single-vessel disease involving 90% stenosis of a nondominant circumflex coronary artery (*3*). Van Hove et al. used 30° LAO first-pass RNA with ^{99m}Tc-pyrophosphate in conjunction with subsequent myocardial infarct imaging to identify the functional consequences of acute infarcts, including those involving the septum and posterolateral wall (*8*).

A study reported by Marshall et al. used first-pass RNA sequentially in the RAO and LAO views to evaluate regional wall motion in eight patients who had also undergone contrast ventriculography (*9*). The RAO first-pass study was first performed with 10 mCi of ^{99m}Tc sulfur colloid, followed by an LAO first-pass study with 15 mCi of

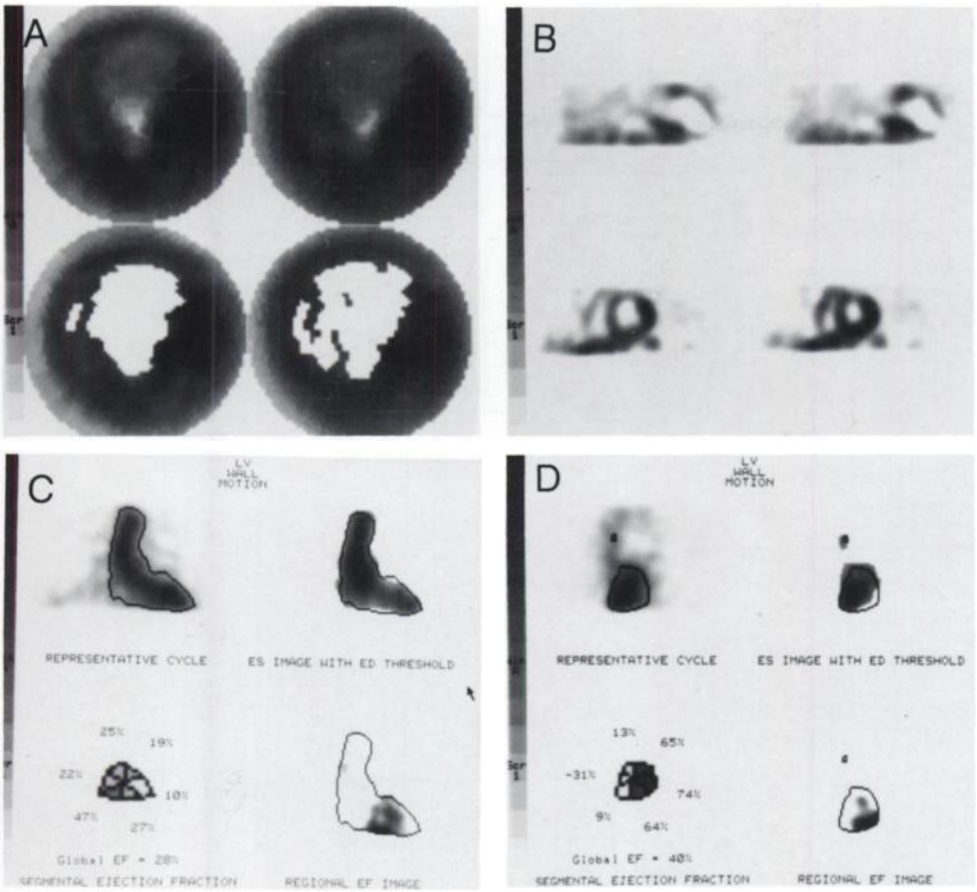

FIGURE 10. Technetium-99m-sestamibi SPECT and biplane first-pass RNA in a patient with an anteroseptal myocardial infarction. (A) Stress (left) and rest (right) raw polar plots (top row) demonstrate an extensive fixed anterior, apical, septal and inferoapical perfusion defect. By quantitative analysis (bottom row) pixels significantly below gender-matched normal limits are highlighted (whitened). (B) End-diastolic (left) and end-systolic (right) tomographic slices demonstrate absent apical wall thickening and hypokinesis with moderately to markedly reduced thickening of the anterior, distal inferior and septal walls. (C) End-diastolic/end-systolic first-pass RNA RAO contours (top right) demonstrate marked hypokinesis to akinesis of the anterior, apical and inferoapical regions. Regional ejection fractions (bottom left) in these areas are markedly reduced. A marked associated abnormality is present in the regional ejection fraction image (bottom left). (D) Analysis of LAO RNA data demonstrates septal akinesis to dyskinesis.

^{99m}Tc-pertechnetate. There was agreement between biplane first-pass RNA and contrast ventriculography in the assessment of regional wall motion in 36 of 40 myocardial segments. Three of the four segments in which there was disagreement were posterolateral.

With the introduction of ^{99m}Tc-labeled myocardial perfusion agents, affording the ability to evaluate both cardiac perfusion and function with a single radiopharmaceutical injection, there has been a recent resurgence of interest in first-pass RNA. There are now several commercially available scintillation camera systems with perpendicular detectors at least theoretically capable of performing simultaneous biplane first-pass RNA. We have demonstrated that with the addition of simultaneous LAO first-pass RNA to conventional RAO imaging, septal and posterolateral wall motion abnormalities can be detected accurately.

In the population we studied, namely patients with coronary artery disease, many with prior myocardial infarcts, the simultaneous biplane RNA technique more accurately characterized the presence and extent of regional wall motion abnormalities. Resting septal and posterolateral wall motion abnormalities occur frequently in patients with coronary artery disease, present in 89% of our patients with abnormal SPECT myocardial perfusion scans. Although not enrolled in our study, in patients with congestive heart failure of unknown etiology, a global evaluation of resting wall motion would be beneficial to distinguish generalized hypokinesis from isolated regional dysfunction, thereby helping to differentiate nonischemic from ischemic cardiomyopathies.

Further development of biplane first-pass RNA may provide additional important advantages. Currently, with only an anterior or RAO view, differentiation of all four cardiac chambers and the temporal sequence of blood flow through them is quite limited. However, orthogonal views in two projections should help to refine the evaluation of these anatomic and hemodynamic relationships, possibly rendering the method more valuable in the assessment of valvular and congenital heart disease. Also, with data acquired simultaneously in two orthogonal planes, the certainty of spatial and temporal localization of scintigraphic events within the cardiac chambers could increase substantially. This could in turn improve image contrast, cardiac chamber boundary definition, edge detection and determination of quantitative parameters such as ejection fraction, volume and regurgitant fraction.

We evaluated only resting ventricular function with first-pass RNA. Other investigators have shown that first-pass imaging at the time of ^{99m}Tc-sestamibi injection can serve as an important adjunct to subsequent SPECT perfusion imaging (*10*). However, the perpendicular two-headed detector system we evaluated requires imaging the patient in the supine (or prone) position. For exercise biplane first-pass RNA, either supine bicycle exercise or pharmacologic

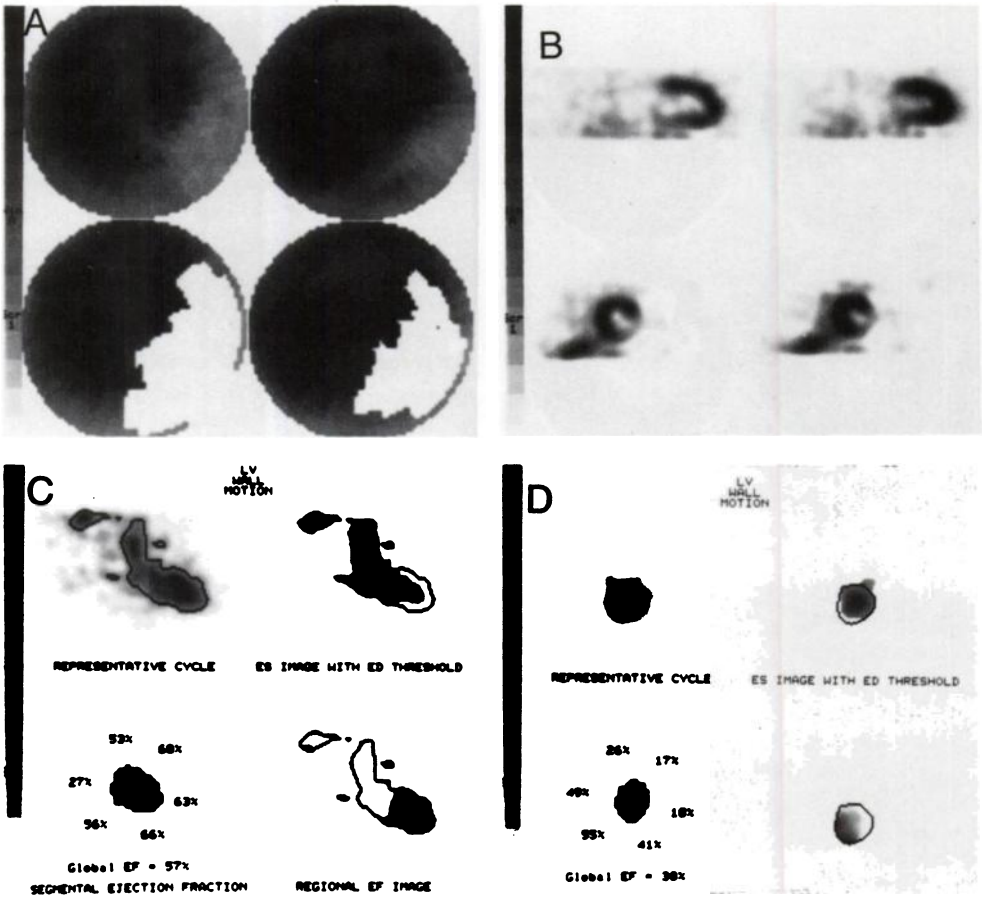

FIGURE 11. Technetium-99m-sestamibi SPECT and biplane first pass RNA in a patient with a clinically "silent" posterolateral myocardial infarction. (A) Stress (left) and rest (right) raw polar plots (top row) and quantitative analysis (bottom row) demonstrate a large posterolateral/inferolateral partially reversible perfusion defect. (B) End-diastolic (left) and end-systolic (right) tomographic slices in the vertical long-axis (top) and short-axis (bottom) projections demonstrate hypokinesis and decreased wall thickening inferobasally and posterolaterally. (C) First-pass RNA in the RAO projection is normal. (D) Analysis of LAO RNA data demonstrates marked posterolateral hypokinesis in the end-diastolic/end-systolic image (top right), decreased posterolateral ejection fractions (bottom left), and a marked associated abnormality in the regional ejection fraction image (bottom right).

(dobutamine or arbutamine) stress would be necessary. At least one commercially available system enables upright biplane imaging, theoretically allowing adequate stress with upright bicycle exercise.

There are a few limitations of the present study. The 60° LAO view used for first-pass RNA occasionally did not allow adequate separation of the left atrium and left ventricle for accurate visual assessment of motion of the posterolateral wall, resulting in two studies that were false positive for posterolateral dysfunction. The effect of left atrial/left ventricular overlap introduced greater error with regard to determining regional ejection fraction. Functional differentiation of normally versus abnormally perfused posterolateral myocardial segments by means of regional ejection fraction was poor. Modified positioning of the perpendicular detectors (i.e., more or less obliquity) or possibly parallel slant hole collimation of the LAO detector (Detector 1) providing a less oblique view of the ventricle, perhaps with a caudal tilt, might serve to better separate the left atrium and left ventricle.

CONCLUSIONS

In summary, simultaneous biplane RAO and LAO first-pass RNA is feasible using a new scintillation camera with two perpendicular detectors. Wall motion abnormalities closely correspond to gated SPECT resting perfusion defects accompanied by decreased wall thickening. With the addition of first-pass LAO RNA to conventional RAO imaging, septal and posterolateral regional asynergy (frequently present in patients with coronary artery disease) can be detected, thereby augmenting the clinical applicability of the method. The technique is particularly well suited to ^{99m}Tc-sestamibi imaging, for which function and perfusion, either at rest or during stress, can be evaluated with a single tracer injection.

REFERENCES

1. Wackers FJT. First-pass radionuclide angiography. In: *Cardiac nuclear medicine.* Gerson MC, ed. New York: McGraw-Hill; 1987.
2. Gal R, Grenier RP, Carpenter J, Schmidt DH, Port SC. High count rate first-pass radionuclide angiography using a digital gamma camera. *J Nucl Med* 1986;27:198–206.
3. Bodenheimer MM, Banka VS, Fooshee C, Gillespie JA, Helfant RH. Detection of coronary heart disease using radionuclide determined regional ejection fraction at rest and during handgrip exercise: correlation with coronary arteriography. *Circulation* 1978;58:640–648.
4. Bodenheimer MM, Banka VS, Fooshee C, Hermann GA, Helfant RH. Relationship between regional myocardial perfusion and the presence, severity and reversibility of asynergy in patients with coronary artery disease. *Circulation* 1978;58:789–795.
5. Nichols K, DePuey EG, Gooneratne N, Salensky H, Friedman M, Cochoff First-pass ventricular ejection fraction using a single-crystal nuclear camera. *J. Nucl Med* 1994;35:1292–1300.
6. Lewellen TK, Bice AN, Pollard KR, Zhu J, Plunkett ME. Evaluation of a clinical scintillation camera with pulse tail extrapolation electronics. *J Nucl Med* 1989;30:1554–1558.
7. Marcassa C, Marzullo P, Parodi O, Sambucetti G, L'Abbate C. A new method for noninvasive quantitation of segmental myocardial wall thicken-

ing using Tc-99m-2-methoxy-isobutyl-isonitrile: scintigraphic results in normal subjects. *J Nucl Med* 1990;31:173–177.
8. Van Hove ED, Heck LL, Kight JL. Improved myocardial infarct localization by combination of scintigraphy and ventricular wall motion evaluation. *Radiology* 1977:124:425–429.
9. Marshall RC, Berger JH, Costin JC, et al. Assessment of cardiac performance with quantitative radionuclide angiocardiography. *Circulation* 1977; 56:820–829.
10. Jones RH, Borges-Neto S, Potts JM. Simultaneous measurement of myocardial perfusion and ventricular function during exercise from a single injection of technetium-99m-sestamibi in coronary artery disease. *Am J Cardiol* 1990;66:68E–71E.